

RSC Advances



This is an *Accepted Manuscript*, which has been through the Royal Society of Chemistry peer review process and has been accepted for publication.

Accepted Manuscripts are published online shortly after acceptance, before technical editing, formatting and proof reading. Using this free service, authors can make their results available to the community, in citable form, before we publish the edited article. This *Accepted Manuscript* will be replaced by the edited, formatted and paginated article as soon as this is available.

You can find more information about *Accepted Manuscripts* in the [Information for Authors](#).

Please note that technical editing may introduce minor changes to the text and/or graphics, which may alter content. The journal's standard [Terms & Conditions](#) and the [Ethical guidelines](#) still apply. In no event shall the Royal Society of Chemistry be held responsible for any errors or omissions in this *Accepted Manuscript* or any consequences arising from the use of any information it contains.

1 **Removal of basic dye Auramine-O by ZnS: Cu nanoparticles loaded on activated carbon**
2 **Optimization of parameters using response surface methodology with central composite**
3 **design**

4 Arash Asfaram^a, Mehrorang Ghaedi^{1a}, Shilpi Agarwal^b, Inderjeet Tyagi^b,
5 Vinod Kumar Gupta^{b,c*}

6 ^a Chemistry Department, Yasouj University, Yasouj 75914-35, Iran.

7 ^b Department of Chemistry, Indian Institute of Technology Roorkee, Roorkee-247 667, India

8 ^c Center for Environment and water, The research Institute, King Fahd university of Petroleum
9 and Minerals Dhahran, Saudi arabia

10

11

12

13

14

15

16

17

18 *Corresponding author. Tel.: +91 1332285801; fax: +91 1332273560.

19 E-mail addresses: vinodfcy@iitr.ac.in, vinodfcy@gmail.com (V.K. Gupta).

20

21 **Abstract**

22 This research is focused on the ultrasound-assisted removal of Auramine-O (AO) dye
23 from aqueous solutions using ZnS:Cu nanoparticles loaded on activated carbon (ZnS:Cu-NP-
24 AC) as an adsorbent. ZnS:Cu nanoparticles were synthesized and characterized using FESEM
25 (Field-Emission Scanning Electron Microscopy) and XRD (X-Ray Diffraction) analysis. The
26 experiments were designed by response surface methodology. Quadratic model was used to
27 predict the variables. Analysis of variance was used for investigation of variables and interaction
28 between them. High F-value (48.91), very low P-value (<0.00001), non-significant lack of fit,
29 the determination coefficient ($R^2 = 0.977$) demonstrate good correlation between experimental
30 and predicted values of the response. The highest removal percent (99.76%) was attained, and
31 the optimum parameters are achieved: adsorbent amount (0.02 g), initial concentration dye (20
32 mgL^{-1}), sonication time (3 min) and $\text{pH}=7$. Adsorption processes of AO by ZnS: Cu-NP-AC
33 could be well described with Langmuir isotherm and a pseudo- second-order kinetic model. The
34 maximum adsorption capacity of AO by ZnS: Cu-NP-AC was determined as 183.15 mg g^{-1} ,
35 suggesting a highly promising potential for ZnS: Cu-NP-AC to be used as a new adsorbent.

36

37

38

39 **Keywords:** Ultrasound-Assisted; Nanoparticle Loaded Activated Carbon; Response Surface
40 Methodology; Auramine-O.

41

42

43

44 **1. Introduction**

45 The discharge of dyes in to the biological ecosystem is worrying for both toxicological
46 and esthetical aspects [1]. Almost 45% of textile dyes produced worldwide belongs to the
47 reactive class [2]. Reactive dyes are common dyes used for dyeing cellulosic fibres due to their
48 favorable characteristics of bright color, water-fastness, simple application techniques and low
49 energy consumption [3]. Auramine-O (AO) and its hydrochloride salts are used as coloring agent
50 in paper, textiles and leather industries [4]. International agency for research on cancer (IARC)
51 included AO among chemicals for which there is sufficient evidence of carcinogenicity due to its
52 bio-transformation to reactive species in target organs of both rats and humans [5, 6]. Auramine-
53 O (AO) is yellow in color and is frequently used in paper mills, textile mills, leather and carpet
54 industry. Presence of these dyes is highly persistent and the manufacturers always go for the
55 most stable dye. For the efficient removal of hazardous impurities, several physical and chemical
56 methods such as coagulation [7], reverse osmosis [8], photo degradation [9], electrochemical
57 oxidation [10], ozonation [11], biosorption [12] and adsorption are used, Among all, adsorption
58 as a popular alternative procedure, especially based on low cost adsorbent benefit from remarks
59 such as, simple design, easy operation and the possibility of using green and non-toxic adsorbent.
60 Many adsorbent were tested on the possibility of the hazardous dye removal such as carbon
61 nanotube [13-21], MWCNTs [22, 23] activated carbon [24, 25], fly ash [26], chitin [27], zeolite
62 [28], polymer [29], low cost adsorbents [30-40], lignin [41, 42], barley straw [43],
63 nanocomposites [44-47] and graphene oxide [48]. Design and application of non-toxic adsorbent
64 that was able to remove a huge amount of hazardous dyes molecule in short time are crucial
65 requirements for the wastewater treatment. Nanoparticles exhibit intrinsic surface activity, high

66 surface areas and reactive atom or functional group strongly chemisorbed many hazardous
67 chemical compounds. The size, surface structure and interparticle interaction of nanomaterials
68 determine their unique properties which proved nanoparticle an efficient adsorbent as well as
69 several other potential applications in many relevant research areas. The key objective of the
70 present work is the synthesis of ZnS:Cu nanoparticle loaded on AC, which is followed by a
71 characterization via different analytical techniques such as UV-vis, SEM and XRD. The
72 potential feasibility of ZnS:Cu-NP-AC for the adsorption process of AO was investigated and
73 the influence of certain variables was studied and optimized by central composite design (CCD)
74 combined with response surface methodology (RSM) using the desirability function (DF) as
75 maximize criterion of the response. The results obtained from the presented models were
76 compared with the experimental values. The adsorption kinetics and isotherms of dye removal on
77 this adsorbent was also investigated. The adsorption rates were evaluated by fitting the
78 experimental data to traditional kinetic models such as pseudo first-order, second-order and
79 intraparticle diffusion models. The proposed sorbent will be useful for quantitative adsorption of
80 the dye with high sorption capacities in short time.

81

82 **2. Materials and methods**

83 ***2.1. Materials and instruments***

84 Auramine-O (4, 4-dimethylaminobenzophenonimide) (AO) were considered as azo dye.
85 Detailed description of this dye is shown in Table 1. The stock solution (200 mg/ L) of dye was
86 prepared by dissolving 200 mg of solid dye in 1000 mL of double distilled water and the
87 working concentrations were prepared daily by suitable dilution. The ZnS: Cu-NP-AC
88 nanoparticles were prepared and characterized by using BET and SEM. The BET (Brunauer,

89 Emmett, and Teller) surface area of the adsorbent material was measured using TriStar II 3020
90 (Micrometrics Instrument Corporation) surface area analyzer where N₂ gas was used as
91 adsorbate. The nitrogen sorption analysis was accomplished using a Belsorp-BEL, Inc. analyzer
92 at 77 K. Prior to measurement, the materials was degassed at 373 K for 12 h. The surface area of
93 the ZnS: Cu-NP-AC was calculated by BET method and the pore size distribution was calculated
94 from the adsorption branch of the isotherm using BJH method. NaOH and HCl with the highest
95 purity were purchased from Merck (Darmstadt, Germany). The pH measurements were carried
96 out using pH/Ion meter model-686 (Metrohm, Switzerland, Swiss) and the AO concentrations
97 were determined using Jasco UV-vis spectrophotometer model V-530 (Jasco, Japan) at
98 wavelength of 434 nm, respectively. An ultrasonic bath with heating system (Tecno-GAZ SPA
99 Ultra Sonic System) at 40 kHz of frequency and 130 W of power was used for the ultrasound-
100 assisted adsorption procedure.

101

102 ***2.2. Ultrasound-assisted adsorption method***

103 A batch method was used to appraise the adsorption performance of AO dye from
104 aqueous solutions onto ZnS: Cu-NP-AC in presence of ultrasonic wave. Adsorption experiments
105 were performed in a cylindrical glass vessel by addition of adsorbent (0.02 g) into 50 mL of AO
106 solutions at known concentration (5 and 30 mg L⁻¹) and pH 7. The vessel was immersed in an
107 ultrasonic bath for 3.0 min sonication time at the room temperature. After this time, solutions
108 were analyzed for the final concentration of dyes by using a UV-vis spectrophotometer set at a
109 wavelength of 434 nm for AO, respectively.

110

111 ***2.3. Measurements of dye uptake***

112 The dye concentrations were determined according to calibration curve obtained at
113 maximum wavelength over functioning concentration range. The efficiency of dye removal was
114 determined at different experimental conditions and optimized according to the CCD method
115 discussed in subsequent section. The dye removal percentage was calculated using the following
116 equation:

$$117 \quad \%R_{JSB} = \frac{C_0 - C_t}{C_0} \times 100 \quad (1)$$

118
119 Where C_0 (mg L^{-1}) and C_t (mg L^{-1}) is the concentration of dye at initial and after time t ,
120 respectively [49].

121

122 **2.4. Kinetic experiments**

123 Kinetic adsorption is performed to investigate the mechanism of adsorption and to
124 determine the equilibrium time [50]. For this purpose 0.01 and 0.02 g of adsorbent was contacted
125 with 50 mL of AO solution with an initial concentration of AO, 10, 20 and 30 mgL^{-1} , in
126 ultrasonic at temperature for different time intervals at the optimum pH 7. The samples were
127 filtered and determined using Jasco UV-vis spectrophotometer model V-530 (Jasco, Japan) at
128 wavelength of 434 nm, respectively [51].

129

130 **2.5. Adsorption isotherms**

131 Adsorption isotherms are used to describe the equilibrium behaviors of adsorbate uptake
132 [52]. For isotherms experiments, various amounts of adsorbents (0.01, 0.015 and 0.02g) were
133 contacted with 50 mL of solution AO with an initial concentration of (5-30 mgL^{-1}), in 6 flasks at
134 the optimum pH 7. The containers were mechanically agitated in a shaker at ultrasonic in room

135 temperature for 3 min. The samples were filtered and determined using Jusco UV-vis
136 spectrophotometer model V-530 (Jasco, Japan) at wavelength of 434 nm, respectively. The
137 adsorbed dye amount (q_e (mg g⁻¹)) was calculated by the following mass balance relationship:

138

$$139 \quad q_e = \frac{(C_0 - C_e)V}{W} \quad (2)$$

140

141 Where q_e is the amount of adsorbed manganese per gram adsorbent at equilibrium (mg/g) and C_0
142 and C_e are the concentrations of the metal ions before and after adsorption (mg/L), V the volume
143 of the aqueous phase (L) and m the mass of the adsorbent (g) [53].

144

145 **2.6. Preparation of ZnS:Cu-NP-AC**

146 Analytical reagent grade zinc sulfate ($ZnSO_4 \cdot 2H_2O$), copper (II) acetate ($Cu(CH_3COO)_2$) and thiourea ($SC(NH_2)_2$) were purchased from Merck company and used without further
147 purification. The preparation of ZnS: Cu-NPs were carried out at two steps. In the first step, ZnS
148 nanoparticles (ZnS-NPs) were synthesized. The precursor solution for synthesis of ZnS-NPs was
149 prepared as follows: 0.6 mmol of zinc sulfate solution was mixed with 30 ml of 0.5M thiourea
150 solution at pH= 5.5 and deionized water was added to the mixed solutions to make a total volume
151 of 250 ml. Then, 250 ml of the precursor solution in a baker was transferred to an autoclave at
152 pressure of 1.25 bar for 3 h. The temperature of the autoclave was 125 °C. After 3 hours, the
153 baker containing the reaction solution containing white colored ZnS-NPs in bottom of the baker
154 was removed from autoclave. The obtained ZnS - NPs were filtered and washed several times by
155 deionized water. In the second step, ZnS: Cu-NPs-AC was prepared. 250 ml of deionized water
156 was added to the ZnS-NPs prepared from step 1 to form an insoluble suspension. 1 ml 0.2 M (Cu

158 (CH₃COO)₂) solution was added to the ZnS-NPs suspension along with vigorous stirring for 5
159 min. After adding Cu²⁺ solution to ZnS-NPs suspension, its color slightly changes from milky
160 white to light green because of the diffusion of Cu²⁺ ions to ZnS-NPs and formation of ZnS: Cu-
161 NPs suspension. Finally, the homogenous deposition of ZnS: Cu-NPs on activated carbon (AC)
162 was carried out by adding 10 g of AC to the obtained ZnS:Cu-NPs suspension and strong stirring
163 for 20 h at room temperature. The prepared ZnS:Cu-NPs-AC were then filtered, washed several
164 times by deionized water, dried at 60 °C for 3h and used as an adsorbent for adsorption
165 experiments, the major impurities that may be present during the synthesis of ZnS:Cu
166 nanoparticles are ZnO and Zn (OH)₂, but the XRD pattern confirm high purity of ZnS:Cu-NP and
167 its agreement with reference material without any further impurity.

168

169 ***2.7. Role of ZnS:Cu nanoparticles***

170 ZnS:Cu nanoparticle poses a crucial role on the adsorption phenomenon, it lead to the
171 enhancement of the surface area and number of active sites, hence it is an efficient adsorbent,
172 when loaded on AC, it causes very rapid adsorption of hazardous materials i.e. dyes, even by
173 using a very low amount of adsorbent dose i.e. 0.02, maximum 99.76% of the adsorption takes
174 place. Hence to carry out at an efficient and maximum adsorption it is needed to coat ZnS:Cu
175 nanoparticles on to the activated carbon because several parameters are effected like sonication
176 time, pH, and adsorbent dose, a major change is reported in the sonication time parameter from
177 120 and 300 minutes it reduces to only 3 minutes to achieve the maximum adsorption.

178 ***2.8. Reusable capacity of ZnS:Cu nanoparticles***

179 Like the other nanoparticles adsorbent i.e. Fe₂O₃ , MnO etc, they can be reused as
180 adsorbent after magnetic separation for removing the noxious toxic contaminants, it is seen that

181 it can be used maximum four times without any change and modification in the developed
182 adsorbent [54, 55]

183 **2.9. Central composite design (CCD)**

184 A central composite design (CCD) was used to determine the optimal conditions for the
185 critical factors. For the adsorption process, significant variables, such as pH, AO concentration,
186 adsorbent and sonication time, were chosen as the independent variables and designated as X_1 –
187 X_4 , respectively. The pH (X_1) ranged from 5 to 9, adsorbent (X_2) ranged from 0.005 to 0.025 g,
188 sonication time (X_3) ranged from 1 to 5 min and the AO concentration (X_4) ranged from 10 to 30
189 mg L^{-1} , as shown in Table 2. The real values of the independent variables (X_i) were coded to z_i
190 according to Eq. (3) by setting the lowest values as -2 and the highest values as +2:

191

$$192 \quad z_i = \frac{x_i - x_0}{\Delta x_i} \quad (3)$$

193

194 Where z_i is the dimensionless value of an independent variable, X_i represents the real value of
195 the independent variable, X_0 is the real value of the independent variable at the center point, and
196 ΔX_i is the step change [56, 57]. The number of experiments was equal to Eq. (4), where k and n
197 are the number of factors and center runs, respectively ($k=4$, $n=7$), plus two additional points. A
198 total of 31 experiments were performed.

199

$$200 \quad N = 2^k + 2k + n_c \quad (4)$$

201

202 Where k is the number of variables and n_c is the number of central points. A four-factor five-
203 level CCD was used to fit the general model of Eq. (5) and to obtain optimal conditions for
204 dependent variables (Y).

205

$$206 \quad y = \beta_0 + \sum_{i=1}^4 \beta_i x_i + \sum_{i=1}^4 \sum_{j=1}^4 \beta_{ij} x_i x_j + \sum_{i=1}^4 \beta_{ii} x_i^2 + \varepsilon \quad (5)$$

207

208 Where y is the response, β_0 , β_i , β_{ii} are the regression coefficients of variables for intercept, linear,
209 quadratic and interaction terms, respectively. X_i and X_j are the independent variables and ε is the
210 residual term. The STATISTICA software (Version 10.0) was used for data processing.
211 Experimental data were fitted to a second-order polynomial equation, and regression coefficients
212 were obtained. The analysis of variance (ANOVA) was performed to justify the significance and
213 adequacy of the developed regression model. The adequacy of the response surface models were
214 evaluated by calculation of the determination coefficient (R^2) and also by testing it for the lack of
215 fit.

216

217 **2. Results and discussion**

218 **3.1. Characterization of adsorbent**

219 The optical absorbance spectrum of the prepared ZnS: Cu–NP–AC has a steep absorption
220 edge, indicating good homogeneity in the shape and size of the particles as well as low defect
221 density near the band edge [64], it is well elucidated from Fig. 1. From the absorption data, the
222 band gap energy of ZnS: Cu–NP–AC was estimated using the well-known relation for
223 semiconductors [58, 59]:

224

$$225 \quad ah\nu = k \left(h\nu - E_g \right)^{\frac{n}{2}} \quad (6)$$

226
227 Where, E_g is the band gap energy, k is a constant, and n is a constant equal to 1 or 4 for direct
228 and indirect band gap materials, respectively. A plot of $(ah\nu)^2$ versus $h\nu$ (inset of Fig. 1) is linear
229 at the absorption edge, which means that the mode of transition in these films has a direct nature.
230 The band gap energy, E_g , was calculated about 3.97 eV from an extrapolation of the straight-line
231 portion of the $(ah\nu)^2$ vs $h\nu$ plot to zero absorption coefficient value. The obtained band gap
232 energy for the prepared ZnS:Cu -NP is larger than that of the bulk ZnS (3.60 eV) which could be
233 assigned to quantum confinement effects in nanosized material.

234 The morphology and particle size of the prepared ZnS:Cu -NP were studied by FESEM (FE-
235 SEM; Hitachi S-4160, Japan) under an acceleration voltage of 200 kV. The FESEM images of
236 the prepared ZnS:Cu -NP at different magnifications were shown in Figs. 2a - 2c. The surface
237 textural and morphology reveals the porous nature and rough surface of the developed adsorbent,
238 it seems that the porous structure was due to the ZnS:Cu nanoparticles loaded on the AC, which
239 should increase the effective surface for adsorption. The XRD patterns of ZnS:Cu nanoparticles
240 prepared at 75 °C has good agreement with standard JCPDS (Joint Committee for Powder
241 Diffraction Standards, JCPDS card No. 05-0566) pattern of ZnS (Fig. 3). The three broad peaks
242 observed in the diffractogram at around 28.56°, 47.93° and 57.12° reveal a cubic lattice structure
243 of (β -ZnS phase) planes (111), (220) and (311), respectively. The broad nature of XRD peaks
244 confirms nanosized particles. According to full width at half-maximum (FWHM) of (110) peak
245 and based on the Debye-Scherrer equation, The average crystalline sizes calculated from the
246 full width at half-maximum (FWHM) of these peaks were about 22 and 21 nm for cubic and
247 hexagonal ZnS:Cu nanoparticles, respectively.

248 3.2. Central composite design (CCD)

249 3.2.1. Model fitting and statistical analysis

250 In the CCD step as presented in Table 2, four independent variables (pH (X_1), adsorbent
251 dosage (X_2), sonication time (X_3) and AO concentration (X_4)) were prescribed into three levels
252 (low, basal and high) with coded value (-1, 0, +1) and the star points of +2 and -2 for + α and - α
253 respectively, were selected for each set of experiments. 31 experiments and their responses are
254 presented in Table 3. In order to optimize AO adsorption, central composite design (CCD) with a
255 total number of 31 experiments was used for the response surface modeling. Step-wise model
256 fitting by STATISTICA 10.0 software was used to get the best fitted model. The software
257 suggested quadratic model by supporting lack of fit and model summary statistics (Table 4). The
258 model adequacy was further checked using ANOVA (Table 4).

259 The ANOVA indicates that the model is highly significant through the F value of 48.91. There is
260 only a 0.01% chance that a “model F value” could occur due to noise. Meanwhile, the p value of
261 the model which is at $p < 0.0001$ also implies that the model is highly significant. The lack of fit
262 value of 3.8065 confirms that the lack of fit is not significant relative to the pure error when $p =$
263 0.057729, which is > 0.05 . The insignificant lack of fit indicates good predictability. The “R-
264 squared” of 0.97717 is in reasonable agreement with the “Adj R-squared” of 0.95719 which also
265 indicates good predictability. Based on data analysis (Table 5), an empirical second order
266 polynomial equation was obtained, which in terms of actual factors is as follows:

$$267$$
$$268 y_{AO} = -91 + 32x_1 - 3x_1^2 + 7730x_2 - 203042x_2^2 - 2x_3^2 - 0.0549x_4^2 + 0.264 x_1x_4 - 32x_2x_4 \quad (7)$$

269

270 Where, y is the percentage removal of AO (%), X_1 , X_2 , X_3 and X_4 are terms for the coded values
271 of pH, adsorbent, sonication time and concentration dye, respectively. (Table 4 according to
272 there should P value of 0.05, it was revealed that pH (X_1), adsorbent dosage (X_2), sonication time
273 (X_3) and concentration dye (X_4), quadratic pH (X_1^2), adsorbent dosage (X_2^2), sonication time (X_3^2)
274 and concentration dye (X_4^2) and pH \times initial AO concentration (X_1X_4) and adsorbent \times initial
275 AO concentration (X_2X_4) are significant model terms. The plot of experimental versus calculated
276 values of removal (%) indicate a good fit (as Fig. 4) and presence of linear relationship between
277 them with high correlation coefficient that indicates normal distribution of error around the mean
278 and good applicability of model for explanation of experimental data. These plots are required to
279 check the normality assumption in fitted model.

280

281 ***3.2.2 Three-dimensional response surface plots***

282 The RSM correspond to CCD model was depicted and considered to optimize the critical
283 factors and describe the nature of the response surface in the experiment. The curvature natures
284 of Fig. 5 show the response surface plots of removal (%) confirm strong interaction between the
285 variables.

286 The three-dimensional response surface plots were used to assigning the interaction between the
287 four variables. The relative impresses of two tested variables on the adsorption efficiency, while
288 maintaining all other variables at fixed levels were illustrated in Fig. 5. Based on the quadratic
289 model, the three-dimensional response surface plots were organized. The optimum situations of
290 the relative variables will resemble with the coordinates of the central point in the upmost level
291 in each of these figures.

292 Fig. 5(a) shows the combined effect of adsorbent and pH on adsorption of AO on ZnS: Cu-NP-
293 AC at constant initial concentration of AO (20 mg/L). It is evident from the figure that pH has a
294 profound effect on removal of AO. With increase in pH, removal of AO decreases at lower
295 amount of ZnS: Cu-NP-AC but at higher amount of ZnS: Cu-NP-AC, removal is almost
296 constant with pH. At constant pH, removal increases with increase in amount of ZnS: Cu-NP-
297 AC. It is quite obvious that when amount of adsorbent is high then removal is also high because
298 available surface area for adsorption is much more.

299 Fig. 5(b) shows response surface plot of the adsorption efficiency as dependent on pH
300 and the sonication time. It seems necessary to mention the surface charge of ZnS: Cu-NP-AC in
301 the pH area under pH_{ZPC} is positive, because of the more H^+ in the solution, and it helps the
302 removal of anionic compounds, but in the pH area over pH_{ZPC} , the ZnS: Cu-NP-AC surface
303 charge is negative due to the presence of OH^- in the solution, and it helps in the removal of
304 cationic compounds (pH area is considered as pH_{ZPC} in spaces, where the catalyst surface charge
305 is zero.). In a low pH, ZnS: Cu-NP-AC has the positive surface charge and adsorbs the
306 compounds with the negative charges like anionic dyes, but when the solution pH is over pH_{ZPC} ,
307 the oxide surface gets the negative charge and can make a complex with cationic compounds. So,
308 according to these considerations, the basic conditions are more ideal for AO dye adsorption
309 because AO dye is a cationic and cationic dye. In basic pH, adsorption happens along with the
310 reduction of dye molecules by ZnS: Cu-NP-AC and in basic pH, adsorption may happen
311 through adsorbing the dye molecules on the ZnS: Cu-NP-AC form.

312 Fig. 5(c) shows the three dimensional response surfaces of the combined effect of initial
313 concentration and pH on percentage removal of dye at constant weight of ZnS: Cu-NP-AC (0.02
314 g). It is evident from the figure that removal of AO decreases when initial concentration

315 increases. Removal attains its maximum value when pH is low and initial concentration is also
316 low.

317 Fig. 5(d) clearly states that as the adsorbent amount and sonication time increases, the
318 adsorption efficiency improves. It could be explained by the fact that the more amounts of ZnS:
319 Cu-NP-AC cause an increase in the adsorbent surface and the active surfaces prepare some
320 spaces for capturing AO dye molecules and increasing these spaces makes the dye get out faster.

321 To study the impact of the dye initial concentration on the adsorption efficiency, some
322 experiments with concentrations (5–25 mg/L) of AO dye and fixed sonication time (2min) and
323 pH (7) were designed and results displayed in Fig. 5(e). The observed decreases in removal
324 percentage at higher initial arrived from lower ratio of vacant sites to candidate dyes molecular
325 that compete for binding to the surface. However at such situation there are not enough spaces
326 for all molecules in high concentration of dye.

327 The effect of initial AO concentration on its removal percentage and its influence on their
328 factors were shown Fig. 5(f). It was seen that in despite of the increase in the amount of dye
329 uptake, its removal efficiency was decreased. At lower dye concentrations, the ratio of solute
330 concentrations to vacant reactive adsorbent sites is lower and accelerates dye adsorption which
331 causes an increase in dye removal. At higher concentrations, lower adsorption yield is due to the
332 saturation of adsorption sites. On the other hand, the percentage removal of dye was higher at
333 lower initial dye concentrations and smaller at higher initial concentrations, which clearly
334 indicate that the adsorption of AO from aqueous solution depend on its initial concentration.

335 ***3.3. Optimization of CCD by DF for extraction procedure***

336 The profile for desirable option with predicted values in the STATISTICA 10.0 software
337 was used for the optimization of the process (Fig. 6). The profile for desirable responses was

338 chosen after specifying the DF for each dependent variable (removal percentage) by assigning
339 predicted values. The scale in the range of 0.0 (undesirable) to 1.0 (very desirable) was used to
340 obtain a global function (D) that its maximum (99.764%) and minimum (60.781%) value
341 concern to JSB adsorption was achieved in this research.

342 Three solutions with different amounts of ideal conditions were used to predict the optimum
343 conditions for AO dye adsorption onto ZnS: Cu-NP-AC (Table 6). The highest removal percent
344 (99.8) achieved in the experiment number 5, compared to the other two experiments. Optimum
345 parameters of the reaction are achieved at pH (7), (0.02 g) of ZnS: Cu-NP-AC, 3 min sonication
346 time and initial concentration (20 mg L⁻¹). The relative deviation coefficient 0.322% concern to
347 RSM experimental design show good agreement and high correlation between actual and
348 predicted amounts and reveal the suitability of empirical model resulted from the design could be
349 used for well describing the relation between factors and the AO dye removal percentage.

350

351 ***3.4. Adsorption equilibrium study***

352 Adsorption properties and equilibrium parameters of each isotherm model indicate the
353 interaction of adsorbent-adsorbate and give comprehensive information about the nature of
354 interaction [60–65]. The widely used isotherm models such as Langmuir, Freundlich, Dubinin
355 and Radushkevich (D-R) and Temkin were used to analyze the experimental equilibrium data
356 obtained from the sorption process at room temperature over the concentration range of 5–30 mg
357 L⁻¹.

358 In the Langmuir isotherm [66], the intermolecular forces decrease rapidly with distance and the
359 predicted monolayer coverage of the adsorbate on the outer surface of the adsorbent is
360 represented in linear form as follows:

361

$$\frac{C_e}{q_e} = \frac{1}{Q_0 k} + \frac{C_e}{Q_0} \quad (8)$$

363

364 A plot $1/q_e$ versus $1/C_e$ should represent a line with slope of $1/Ka Q_m$ and $1/Q_m$ intercept of $1/Q_m$
365 and respective data are presented in Table 7. The high correlation ($R^2 > 0.999$) coefficient shows
366 that Langmuir isotherms are applicable for the interpretation of AO adsorption onto ZnS: Cu-
367 NP-AC over the whole concentration range studies and maximum adsorption capacity of 92.26 –
368 183.15 mgg^{-1} .

369

370 The data was analyzed by the linearized form of Freundlich isotherm model:

$$\ln q_e = \ln K_F + \frac{1}{n} \ln C_e \quad (9)$$

372 Where q_e is the amount of adsorption, k_f is the Freundlich constant related to sorption
373 capacity and $1/n$ is a constant related to energy or intensity of adsorption. This gives an
374 expression encompassing the surface heterogeneity and the exponential distribution of
375 activated sites and their energies. This isotherm does not predict any saturation of the
376 adsorbent surface. The Freundlich exponent's k_f and $1/n$ can be determined from the linear plot
377 of $\log q_e$ vs. $\log C_e$. The values of the Freundlich constants K_f and $1/n$ are 4.982-5.559 and
378 0.4544-1.130 respectively shown in Table 7. The slope $1/n$ ranging between 0 and 1 is a
379 measure of adsorption intensity or surface heterogeneity, becoming more heterogeneous
380 as its value gets closer to zero [67].

381 Table 7 shows that Langmuir model fits for AO dye (correlation coefficient 0.990-0.998)
382 adsorption process. Heat of adsorption and the adsorbent-adsorbate interaction on adsorption

383 isotherms were studied by Temkin [68], its equation is given as:

$$384 \quad q_e = B \ln K_T + B \ln C_e \quad (10)$$

385 where $B_T = RT/b$, T is the absolute temperature in K, R the universal gas constant, 8.314 J
386 $\text{mol}^{-1} \text{ K}^{-1}$, K_T the equilibrium binding constant (L mg^{-1}) and B is related to the heat of
387 adsorption. The constants obtained for Temkin isotherm are shown in Table 7.

388 The linear form of Dubinin-Radushkevich isotherm equation can be expressed as [69].

$$389 \quad \ln q_e = \ln Q_S - B\varepsilon^2 \quad (11)$$

390 The plot of $\ln q_e$ vs. ε^2 at different temperatures for AO is presented. The constant obtained for
391 D–R isotherms are shown in Table (7). The mean adsorption energy (E) gives information
392 about chemical and physical nature of adsorption [70].

393 The values of the parameters of the three isotherms and their related correlation coefficients are
394 shown in Table 7, the Langmuir model yields a somewhat better fit ($R^2 = 0.990\text{-}0.998$), Temkin
395 isotherm ($R^2=0.925\text{-}0.986$) than the Freundlich model ($R^2 = 0.787\text{-}0.910$) and Dubinin-
396 Radushkevich model ($R^2 = 0.913\text{-}0.984$). Equilibrium data fitted well with the Langmuir model.

397

398 **3.5. Kinetic study**

399 Adsorption of a solute by a solid in aqueous solution usually occurs with a complex
400 kinetics [71]. The adsorption rate is strongly influenced by several parameters related to the state
401 of the solid (generally with very heterogeneous reactive surface) and to physico-chemical
402 conditions under which the adsorption is occurred. To investigate the adsorption processes of AO
403 on the adsorbent, pseudo-first-order and pseudo-second-order adsorption were studied. The

404 Lagergren pseudo-first-order model described the adsorption kinetic data [72]. The Lagergren
405 equation is commonly expressed as follows:

$$406 \frac{dq_t}{dt} = k_1(q_e - q_t) \quad (11)$$

408
409 Where q_e and q_t (mg/g) are the adsorption capacities, at equilibrium and at time t respectively. k_1
410 is the rate constant of the pseudo-first-order adsorption (L/min). From the following model, plot
411 of $\log(q_e - q_t)$ versus t was made and the values of k_1 and q_e were determined by using the slope
412 and intercept of the plot, respectively.

$$413 \log(q_e - q_t) = \log q_e - \left(\frac{k_1}{2.303}\right)t \quad (12)$$

415
416 The fact that the intercept is not equal to q_e , means that the reaction unlikely follows the first-
417 order, regardless of the value of correlation coefficient [73]. The variation in rate should be
418 proportional to first power of concentration for strict surface adsorption. However, the
419 relationship between initial solute concentration and rate of adsorption is linear when pore
420 diffusion limits the adsorption process. Furthermore, the correlation coefficient, R^2 is relatively
421 low for most adsorption data (See Table 8). This indicates that the adsorption of AO onto
422 ZnS:Cu -NP-AC was not a first-order reaction. Therefore, it is necessary to fit experimental data
423 to another model. The adsorption kinetic may be described by the pseudo-second order model
424 [74], which is generally given by the following equation:

425

426
$$\frac{dq_t}{dt} = k_2(q_e - q_t)^2 \quad (13)$$

427

428 Eq. (13) is integrated over the interval 0 to t for t and 0 to q_t for q_t , to give

429

430
$$\frac{t}{q_t} = \frac{1}{k_2 q_e^2} + \frac{t}{q_e} \quad (14)$$

431 As mentioned above, the plot of $\log(q_e - q_t)$ versus t does not show good results for entire
432 sorption period, while the plot of t/q_t versus t shows a straight line. The values of k_2 and
433 equilibrium adsorption capacity (q_e) were calculated from the intercept and slope of the plot of
434 t/q_t versus t (Table 8). For all concentrations and sorbent doses, the calculated q_e values were
435 mainly close to the experimental data and R^2 values for the pseudo-second-order kinetic model
436 were found to be larger than that for the pseudo-first-order kinetic. This indicates that the
437 pseudo-second-order kinetic model applies better for the adsorption of AO dye for the entire
438 sorption period. The intraparticle diffusion equation is given as [75]:

439

440
$$q_t = K_{dif} t^{1/2} + C \quad (15)$$

441

442 Where K_F is the intraparticle diffusion rate constant ($\text{mg} (\text{gmin}^{1/2})^{-1}$) and C shows the boundary
443 layer thickness. The linear form of Elovich model equation is generally expressed as [76]:

444

445
$$q_t = \frac{1}{\beta} \ln(\alpha\beta) + \frac{1}{\beta} \ln t \quad (16)$$

446

447 The kinetic data from pseudo-first and pseudo-second-order adsorption kinetic models and the
448 intraparticle diffusion and Elovich model are given in Table 8. The linear plots of t/q_t versus t
449 indicated a good agreement between the experimental and calculated q_e values for different
450 initial dye concentrations. Furthermore, the correlation coefficients of the pseudo-second-order
451 kinetic model ($R^2 \geq 0.999$) were greater than that of the pseudo-first-order model ($R^2 \leq 0.983$). As a
452 result, it can be said that the adsorption fits to the pseudo-second-order better than the pseudo-
453 first-order kinetic model.

454

455 **3.6. Comparison with other methods**

456 The ZnS: Cu–NP–AC prepared in this work had a relatively large adsorption capacity on
457 AO compared to some other adsorbents reported in the literature, primarily when ZnS: Cu loaded
458 on AC, it lead to rapid decrease in contact time parameter, it is reported that time taken by
459 activated carbon is about 120 minutes [77], time taken by graphite loaded with titania is about
460 300 minutes [78], but when AC loaded with ZnS:Cu nanoparticle time taken by the adsorbent
461 rapidly decrease and it takes nearly 3 minutes to adsorb the maximum amount of Auramine –O .
462 Secondly the maximum amount of the adsorbate adsorbed on the adsorbent also increases form
463 1.509 mg/g (for AC) it becomes 94.26 mg/g (for ZnS:Cu nanoparticles loaded on AC)

464 Table 9 lists the comparison of maximum monolayer adsorption capacity of AO on various
465 adsorbents. The adsorption capacity and contact time for proposed method in comparison with
466 all of the adsorbents are preferable and superior to the literature which shows satisfactory
467 removal performance for AO as compared to other reported adsorbents [77- 80]. The results
468 indicated that the ultrasound assisted removal method has a remarkable ability to improve the
469 removal efficiency of dyes. The ultrasonic-assisted enhancement of removal could be attributed

470 to the high-pressure shock waves and high-speed microjets during the violent collapse of
471 cavitation bubbles [81, 82].

472 **4. Conclusion**

473 The results of the present studies showed that ZnS: Cu-NP-AC prepared by synthesis
474 method was an efficient adsorbent for the Auramine-O removal. The use of response surface
475 methodology involving central composite design for optimization of process parameters was
476 studied. Experiments were performed as a function of initial pH, dye concentration, sonication
477 time and adsorbent dosage, these factors are well studied and optimized. The optimized values,
478 at which the highest removal percent (99.76%) was attained, are achieved: pH=7, initial
479 concentration dye (20 mgL^{-1}), sonication time (3 min) and adsorbent amount (0.02 g). In the
480 present study, the analytical utility of experimental design for evaluation of optimum condition
481 for the removal of AO in aqueous solution by ZnS: Cu-NP-AC coupled with ultrasound assisted
482 adsorption method has been investigated. The equilibrium and kinetic studies were investigated
483 for the adsorption process. The isotherm models such as Langmuir, Freundlich, Temkin, and
484 Dubinin-Radushkevich were evaluated and the equilibrium data were best described by the
485 Langmuir model. The high correlation ($R^2 > 0.999$) coefficient shows that Langmuir isotherms are
486 applicable for the interpretation of AO adsorption onto ZnS: Cu-NP-AC over the whole
487 concentration range studies and maximum adsorption capacity of $92.26 - 183.15 \text{ mgg}^{-1}$. The
488 process kinetics can be successfully fitted to the pseudo-second-order kinetic model.

489

490 **Acknowledgement**

491 The authors express their appreciation to the Graduate School and Research Council of
492 the University of Yasouj for financial support of this work.

493 **References**

- 494 [1] H.M. Pignon, C.F. Brasquet, P.L. Cloirec, *Sep. Purif. Technol.* 31 (2003) 3–11.
- 495 [2] O. Tunc, H. Tanac, Z. Aksu, *J. Hazard. Mater.* 163 (2009) 187–198.
- 496 [3] S. Dutta, A. Bhattacharyya, A. Ganguly, S. Gupta, S. Basu, *Desalination* 275 (2011) 26–36.
- 497 [4] A. Martelli, G.B. Campart, R. Canonero, R. Carrozzino, F. Mattioli, L. Robbiano, M.
498 Cavanna, *Mutat. Res.* 414 (1998) 37–47.
- 499 [5] ARC, *Monographs on the Evaluation of Carcinogenic Risk to Humans, Supplement 7:*
500 *Overall Evaluations of Carcinogenicity: an Updating of IARC Monographs, vols. 1–42,*
501 *International Agency for Research on Cancer, Lyon, France, 1987, pp. 118–119.*
- 502 [6] A. Dabrowski, *Advances in Colloid and Interface Science.* 93 (2001) 135-224.
- 503 [7] O. Tunay, I. Kabdasli, G. Eremektar, D. Orhon, *Water Science and Technology* 34 (1996)
504 9-16.
- 505 [8] E. Forgacs, T. Cserha' ti, G. Oros, *Environment International* 30 (2004) 953-971.
- 506 [9] K. Wu, Y.X.J. Zhao, H. Hidaka, *Journal of Molecular Catalysis A: Chemical* 144 (1999)
507 77-86.
- 508 [10] E. Kusvuran, O. Gulnaz, S. Irmak, O.M. Atanur, H.I. Yavuz, O. Erbatur, *Journal of*
509 *Hazardous Materials* 109 (2004) 85-93.
- 510 [11] T. Robinson, G. McMullan, R. Marchant, P. Nigam, *Bioresource Technology* 77 (2001)
511 247-255.
- 512 [12] M. Ghaedi, A.G. Nasab, S. Khodadoust, M. Rajabi, , S. Azizian, *Journal of Industrial and*
513 *Engineering Chemistry*, 20(2014) 2317-2324.
- 514 [13] H. Mahmoodian, O. Moradi, B. Shariatzadeha, T.A. Saleh, I. Tyagi, A. Maity, M. Asif,
515 V. K. Gupta, *Journal of Molecular Liquids*, 202, (2014), 189–198.

- 516 [14] B. J. Sanghavi, S. Sitaula, M. H. Griep, S. P. Karna, M. F. Ali, N. S. Swami, *Analytical*
517 *chemistry* 85, 2013, 8158-8165.
- 518 [15] B. J. Sanghavi, S. M. Mobin, P. Mathur, G. K. Lahiri, A. K. Srivastava, *Biosens.*
519 *Bioelectron*, 2013, 39, 124-132.
- 520 [16] B. J. Sanghavi, W. Varhue, J. L. Chávez, C.F Chou, N. S. Swami, *Anal. Chem* 86
521 (2014) 4120-4125.
- 522 [17] B. J. Sanghavi, A. K. Srivastava, *Electrochimica Acta* 55, 2010, 8638-8648.
- 523 [18] B. J. Sanghavi, O. S. Wolfbeis, T. Hirsch, N. S. Swami, *Microchimica Acta* 182
524 (2015) 1-41.
- 525 [19] S. Wang, C. W. Ng, W. Wang, Q. Li, L. Li, *J. Chem. Eng. Data*, 2012, 57, 1563-1569.
- 526 [20] T. A. Saleh, V. K. Gupta, *Environ Sci Pollut Res*, 19 (2012) 1224-1228.
- 527 [21] V. K. Gupta, S. Agarwal, T. A. Saleh, *J. Hazardous Mat.* 185 (2011) 17-23.
- 528 [22] H. Khani, M. K. Rofouei, P. Arab, V. K. Gupta, Z. Vafaei, *J. Hazardous Materials*, 183
529 (2010)402-409.
- 530 [23] T. A. Saleh, V. K. Gupta, *J. Colloids Interface Sci.*, 371 (2012)101-106.
- 531 [24] A. R. Dinçer, Y. Güneş, N. Karakaya, E. Güneş, *Bioresource technology*, 98, (2007), 834-
532 839.
- 533 [25] T. E. Köse, H. Demiral, N. Öztürk, *Desalination and Water Treatment*, 29, (2011), 110-118.
- 534 [26] P. Janoš, H. Buchtová, M. Rýznarová, *Water research*, 37, (2003), 4938-4944.

- 535 [27] G. McKay, H. S. Blair, J. R. Gardner, *Journal of Applied Polymer Science*, 27, (1982),
536 3043-3057.
- 537 [28] S. K. Alpat, Ö. Özbayrak, Ş. Alpat, H. Akçay, *Journal of hazardous materials*, 151, (2008),
538 213-220.
- 539 [29] G. Crini, *Dyes and Pigments*, 77, (2008), 415-426.
- 540 [30] I. Ali, V.K. Gupta, *Advance in water treatment by adsorption technology*, *Nat. Protoc.* 1
541 (2006) 2661–2667.
- 542 [31] I. Ali, *Sep. & Purif. Rev.*39, (2010), 95-171.
- 543 [32] I. Ali, *Chem. Revs. (ACS)*,112: (2012), 5073-5091.
- 544 [33] I. Ali, M. Asim, T. A. Khan, *J. Environ. Manag.*, 113: (2012), 170-183.
- 545 [34] I. Ali, *Seprn. & Purfn. Rev.*, 43: (2014), 175-2015.
- 546 [35] V. K. Gupta, A. Mittal and J. Mittal, *J. Colloid Interface Sci.*, 344, (2010) 497-507.
- 547 [36] V. K. Gupta, S. K. Srivastava. D. Mohan and S. Sharma, *Waste Management*, 17(1998)
548 517-522.
- 549 [37] V. K. Gupta, A. Mittal and J. Mittal, *J. Colloid Interface Sci.*, 342(2010)518-527.
- 550 [38] V. K. Gupta, A. Mittal, D. Kaur A. Malviya, J. Mittal, *J. Colloid Interface Sci.*,
551 337(2009)345-354.
- 552 [39] V. K. Gupta, I. Ali, T. A. Saleh, A. Nayak, S. Agarwal, *RSC Advances* 2 (2012), 6380 –
553 6388.
- 554 [40]A. Mittal, A. Malviya and J. Mittal, V. K. Gupta, *J. Colloid Interface Sci.*, 340(2009) 16-26.

- 555 [41] P.J.M. Carrott, Suhas, M.M.L. Ribeiro Carrott, C.I. Guerrero, L.A. Delgado, Journal of
556 Analytical and Applied Pyrolysis, 82, (2008), 264-271.
- 557 [42] Suhas, P.J.M. Carrott, M.M.L. Ribeiro Carrott, Carbon, 47, (2009), 1012-1017.
- 558 [43] B.C. Oei, S. Ibrahim, S. Wang, H.M. Ang, Biores. Technol., 2009, 100, 4292-4295.
- 559 [44] Y. Yao, S. Miao, S. Liu, L. P. Ma, H. Sun, S. Wang, Chem. Eng. J., 2012, 184, 326-
560 332.
- 561 [45] V. K. Gupta, R. Jain, A. Mittal, S. Agarwal, S. Sikarwar, Materials Science and
562 Engineering: C, 32 (2012)12-17.
- 563 [46] V. K. Gupta and A. Nayak, Chem. Eng. J., 180(2012) 81-90
- 564 [47] V. K. Gupta, R. Jain, S. Agarwal, and M. Shrivastava, Materials Science and Engineering: C
565 31 (2011) 1062-1067.
- 566 [48] P. Bradder, S. K. Ling, S. Wang, S. Liu, J. Chem. Eng. Data, 2011, 56, 138-141.
- 567 [49] A. Shamsizadeh, M. Ghaedi, A. Ansari, S. Azizian, M.K.Purkait, Journal of Molecular
568 Liquids, 195 (2014) 212-218.
- 569 [50] Y. Liu, Colloids and Surfaces A: Physicochemical and Engineering Aspects 274 (2006) 34-
570 36.
- 571 [51] M. Ravanan, M. Ghaedi, , A. Ansari, F. Taghizadeh, , D. Elhamifar, Spectrochimica Acta
572 - Part A: Molecular and Biomolecular Spectroscopy, 123 (2014) 467-472.
- 573 [52] J.R. Utrilla, I.B. Toledo, M.A.F. Garcy, C. Moreno, Journal of Chemical Technology and
574 Biotechnology 76 (2001) 1209-1215.

- 575 [53] A. Omri, M. Benzina, Alexandria Engineering Journal 51(2012)343-350.
- 576 [54] Y. G. Zhao, H. Y. Shen, S. D. Pan, M. Q. Hu, Q. H. Xia, J. Mater. Sci. **45**(19), 5291-5301
577 (2010)
- 578 [55] L. Wang, J. Li, Q. Jiang, L. Zhao, Dalton Trans. **41**(15), 4544-4551 (2012)
- 579 [56] V. Gunaraj, N. Murugan, J. Mater. Process. Technol. 88(1999) 266–275.
- 580 [57] A.R. Khataee, M. Zarei, M. Fathinia, M. Khobnasab Jafari, Desalination 268 (2011) 126–
581 133.
- 582 [58] A. Goudarzi, G. Motedayen Aval, R.Sahraei, H. Ahmadpoor, Thin Solid Films. 516
583 (2008) 4953–4957.
- 584 [59] S.D. Sartale, B.R. Sankapal, M.L. Steiner, A. Ennaui, Thin Solid Films. 480 (2005) 168-
585 172.
- 586 [60] R. Liu, B. Zhang, D. Mei, H. Zhang, J. Liu, Desalination 268 (2011) 111-116
- 587 [61] N. Kannan, M.M. Sundaram, Dyes and Pigments 51 (2001) 25-40.
- 588 [62] I. Langmuir, Journal of the American Chemical Society 38 (1916) 2221-2295.
- 589 [63] A. Asfaram, M.R. Fathi, S. Khodadoust, M. Naraki, Spectrochimica Acta Part A:
590 Molecular and Biomolecular Spectroscopy, 127 (2014) 415-421.
- 591 [64] M. Ghaedi, M. Pakniat, Z. Mahmoudi, S. Hajati, R. Sahraei, A. Daneshfar,
592 Spectrochimica Acta - Part A: Molecular and Biomolecular Spectroscopy, 123 (2014) 402-
593 409.
- 594 [65] A. Mittal, D. Kaur, J. Mittal, Journal of Colloid and Interface Science 326 (2008) 8-17.
- 595 [66] M. Ghaedi, H. Tavallali, M. Sharifi, S. Nasiri Kokhdan, A. Asghari, Spectrochimica Acta
596 Part A 86 (2011)107-114.
- 597 [67] F. Haghseresht, G. Lu, Energy Fuels 12 (1998) 1100-1107.

- 598 [68] M.J. Temkin, V. Pyzhev, *Acta Physiochimica USSR* 12 (1940) 217-222.
- 599 [69] M.M. Dubinin, L.V. Radushkevich, *Chem. Zentr* 1(1947) 875-889
- 600 [70] G. Renmin, S. Yingzhi, C. Jian, L. Huijun, y. Chao, *Dyes and Pigments* 67 (2005) 175-181
- 601 [71] M.J. Culzoni, A.V. Schenone, N.E. Llamas, M. Garrido, et.al. *J. Chromatogr. A* 1216
602 (2009) 7063-7070.
- 603 [72] R.S. Juang, F.C. Wu, R.L. Tseng, *Environ. Technol.* 18 (1997) 525-531.
- 604 [73] T. Robinson, G. McMullan, R. Marchant, P. Nigam, *Bioresour. Technol.* 77 (2001) 247-
605 255.
- 606 [74] M.R. Fathi, A. Asfaram, A. Farhangi, *Spectrochimica Acta Part A: Molecular and*
607 *Biomolecular Spectroscopy*, 135(2015) 364-372.
- 608 [75] J. R. Weber, W. J., J. C. Morris, *Journal of Sanitary Engineering Division ASCE*, 89 (1963)
609 31-59.
- 610 [76] Y.S. Ho, G. McKay, *Biochem.* 34 (1999) 451-465.
- 611 [77] I. D. Mall, V. C. Srivastava, N. K. Agarwal, *J. Hazard. Mater.* 143 (2007) 386–395.
- 612 [78] X-Yan Pang, *E-Journal of Chemistry.* 8(4) (2011) 1644-1653.
- 613 [79] J. Pal, M. K. Deb, *Appl Nanosci* (2014) 4:967–978.
- 614 [80] J. Pal, M. K. Deb, D. K. Deshmukh, D. Verma, *Appl Water Sci* (2013) 3:367–374.
- 615 [81] S.R. Shirsath, D.V. Pinjari, P.R. Gogate, S.H. Sonawane, A.B. Pandit, *Ultrason. Sonochem.*
616 20 (2013) 277–286.
- 617 [82] P.R. Gogate, V.S. Sutkar, A.B. Pandit, *Chem. Eng. J.* 166 (2011) 1066–1082.

618

619

620

621 **Figure captions:**

622 **Fig. 1.** UV-vis absorbance spectrum of the prepared ZnS:Cu-NP-AC (inset: Plot of $(ah\nu)^2$ vs.
623 $(h\nu)$ for the prepared ZnS:Cu-NP-AC)

624 **Fig. 2.** FESEM images of the prepared ZnS:Cu-NPs-AC.

625 **Fig. 3.** XRD pattern for prepared ZnS: Cu-AC-NP. (H: hexagonal and C: cubic)

626 **Fig. 4.** The experimental data vs predicted data for removal of AO.

627 **Fig. 5.** Response surfaces for the AO removal: (a) X_1 - X_2 ; (b) X_1 - X_3 (c) X_1 - X_4 (d) X_2 - X_3 ; (e) X_2 -
628 X_4 and (f) X_3 - X_4 .

629 **Fig. 6.** Profiles for predicated values and desirability function for removal percentage of AO.
630 Dashed line indicated current values after optimization.

631

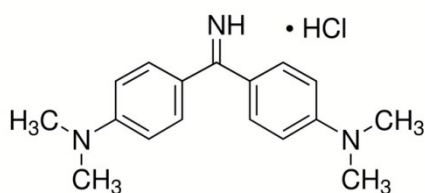
632

633

634 **Table 1**

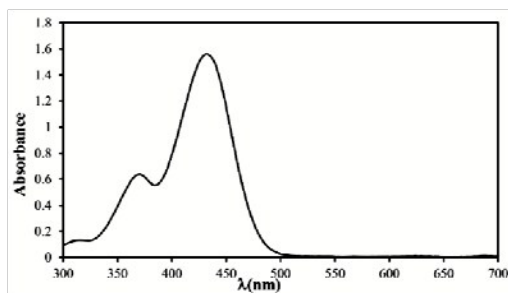
635 Properties of the Auramine-O

Color index number	41000
CAS number	2465-27-2
Chemical Formula	C ₁₇ H ₂₁ N ₃ .HCl
Molecular weight (g mol ⁻¹)	303.83
Maximum wavelength(λ_{\max}), nm	434



Molecular Structure

Absorption spectrum



Type of dye

Basic Yellow (Cationic)

Use

paper mills, textile mills, leather and carpet industry

636

637

638

639

640

641

642 **Table 2**

643 Design matrix for the central composite designs.

Factors	Levels				
	Low (-1)	Central(0)	High(+1)	- α	+ α
X ₁ : Ph	6	7	8	5	9
X ₂ : Adsorbent (g)	0.01	0.015	0.02	0.005	0.025
X ₃ : time (min)	2	3	4	1	5
X ₃ : AO concentration (mg L ⁻¹)	15	20	25	10	30

644

645

646

647

648

649

650

651

652

653

654

655

656

657

658

659 **Table 3**

660 Design matrix for the CCD

Run	X ₁	X ₂	X ₃	X ₄	%Removal Auramine-O	
					Observed ^a	Predictd ^b
1	7	0.015	3	10	94.98000	94.5652
2	6	0.020	2	15	96.78000	97.5729
3	7	0.005	3	20	60.78000	61.5518
4	7	0.025	3	20	96.78000	93.3768
5	8	0.010	2	25	73.97000	73.4753
6	6	0.010	4	25	81.56000	82.5158
7	9	0.015	3	20	81.89000	81.0778
8	6	0.020	4	25	95.80000	96.9945
9(C)	7	0.015	3	20	98.50000	97.7686
10(C)	7	0.015	3	20	98.67000	97.7686
11	6	0.020	4	15	99.76000	102.584
12	8	0.020	2	25	85.36000	87.6090
13	8	0.010	4	15	75.93000	77.8486
14	8	0.020	4	25	94.56000	96.3253
15	5	0.015	3	20	92.42300	90.6038
16(C)	7	0.015	3	20	98.10000	97.7686
17	8	0.010	2	15	73.35000	72.4574
18(C)	7	0.015	3	20	97.60000	97.7686
19	6	0.010	2	15	80.75000	81.3141

20	6	0.020	2	25	89.68000	90.0908
21(C)	7	0.015	3	20	97.98000	97.7686
22(C)	7	0.015	1	20	86.67000	85.2468
23	8	0.020	2	15	88.43000	89.8036
24(C)	7	0.015	3	20	95.08000	97.7686
25	7	0.015	3	30	92.21000	89.9935
26	7	0.015	3	20	98.45000	97.7686
27	6	0.010	4	15	86.84000	84.8929
28	8	0.020	4	15	97.80000	96.6274
29	8	0.010	4	25	81.25000	80.7590
30	7	0.015	5	20	98.75000	97.5418
31	6	0.010	2	25	75.57000	77.0445

661 C: Center point

662 ^a Experimental values of response.

663 ^b Predicted values of response by RSM proposed model.

664

665

666

667

668

669

670

671

672

673 **Table 4**

674 Analysis of variance (ANOVA) for CCD (AO)

Source of variation	Sum of square	Df ^a	Mean square	F-value	P-value	
X_1	136.117	1	136.117	88.5478	0.000082	*
X_1^2	254.271	1	254.271	165.4105	0.000014	*
X_2	1519.246	1	1519.246	988.3111	0.000000	*
X_2^2	736.809	1	736.809	479.3143	0.000001	*
X_3	226.751	1	226.751	147.5074	0.000019	*
X_3^2	72.617	1	72.617	47.2393	0.000468	*
X_4	31.350	1	31.350	20.3942	0.004035	*
X_4^2	53.852	1	53.852	35.0325	0.001036	*
X_1X_2	1.183	1	1.183	0.7694	0.414155	**
X_1X_3	3.285	1	3.285	2.1371	0.194089	**
X_1X_4	27.958	1	27.958	18.1872	0.005294	*
X_2X_3	2.052	1	2.052	1.3349	0.291861	**
X_2X_4	10.320	1	10.320	6.7135	0.041154	*
X_3X_4	3.582	1	3.582	2.3299	0.177762	**
Lack-of-Fit	58.514	10	5.851	3.8065	0.057729	**
Pure Error	9.223	6	1.537			
Total	2966.557	30	136.117			

675 ^a Degree of freedom * Significant

** Not significant

676 **Table 5**

677 Regression coefficients (AO)

Factor	Regressn	Std.Err.	T	P
Mean/Interc.	-91	19.151	-4.7349	0.003208
X_1	32	3.724	8.5673	0.000139
X_1^2	-3	0.232	-12.8612	0.000014
X_2	7730	603.619	12.8053	0.000014
X_2^2	-203042	9274.201	-21.8932	0.000001
X_3	6	3.018	2.1525	0.074851
X_3^2	-2	0.232	-6.8731	0.000468
X_4	0	0.631	0.4987	0.635739
X_4^2	-0	0.009	-5.9188	0.001036
X_1X_2	54	61.992	0.8771	0.414155
X_1X_3	0	0.310	1.4619	0.194089
X_1X_4	0	0.062	4.2646	0.005294
X_2X_3	72	61.992	1.1554	0.291861
X_2X_4	-32	12.398	-2.5911	0.041154
X_3X_4	0	0.062	1.5264	0.177762

678

679

680

681 **Table. 6**

682 Optimum conditions derived by RSM design for dye removal.

Exp.	Optimal conditions				Removal%		
	pH	Adsorbent (g)	Sonication time (min)	AO Concentration (mg L ⁻¹)	Predicted value	Predicted value	RSE%
1	7.0	0.02	3.0	20	99.671	100	0.329
2	7.0	0.02	3.0	20	99.542	100	0.458
3	7.0	0.02	3.0	20	98.877	100	1.123
4	7.0	0.02	3.0	20	99.678	100	0.322
5	7.0	0.02	3.0	20	98.321	100	1.679

683

684

685

686

687

688

689

690

691

692

693

694

695

696 **Table 7**

697 Various isotherm constants and correlation coefficients calculated for the adsorption of
 698 Auramine-O onto ZnS: Cu-NP-AC.

Isotherm	Parameters	Value of parameters		
		0.01 g	0.015 g	0.02 g
Langmuir	Q_m ($\text{mg}\cdot\text{g}^{-1}$)	183.15	122.54	94.26
	K_a ($\text{L}\cdot\text{mg}^{-1}$)	0.402	0.8111	1.102
	R^2	0.990	0.994	0.998
Freundlich	$1/n$	0.4544	0.4121	0.382
	K_F ($\text{L}\cdot\text{mg}^{-1}$)	5.559	5.318	4.982
	R^2	0.864	0.787	0.910
Temkin	B_1	59.697	23.884	16.69
	K_T ($\text{L}\cdot\text{mg}^{-1}$)	5.0964	10.665	18.56
	R^2	0.984	0.925	0.986
Dubinin-Radushkevich	Q_s ($\text{mg}\cdot\text{g}^{-1}$)	138.29	103.99	71.95
	$B\times 10^{-7}$	2.23	1.4	1.00
	E	1497	1889	2236
	R^2	0.960	0.984	0.913

699

700

701

702

703

704 **Table 8**

705 Kinetic parameters for the adsorption of Auramine-O onto ZnS: Cu-NP-AC adsorbents.

Model	Parameters	Value of parameters					
		0.01 g			0.02 g		
		10	20	30	10	20	30
		mg L ⁻¹	mg L ⁻¹	mg L ⁻¹	mg L ⁻¹	mg L ⁻¹	mg L ⁻¹
First-order kinetic	$k_1(\text{min}^{-1})$	0.0145	0.0131	0.0175	0.016	0.0135	0.024
	$q_e(\text{calc})(\text{mg g}^{-1})$	3.907	5.844	8.385	7.23	11.716	25.14
	R^2	0.969	0.983	0.922	0.972	0.863	0.965
Pseudo-second-order kinetic	$k_2(\text{min}^{-1})$	0.001	0.0003	0.00018	0.004	0.0021	0.002
	$q_e(\text{calc})(\text{mg g}^{-1})$	49.75	102.04	147.06	25.12	48.309	65.56
	R^2	0.999	0.998	0.997	0.999	0.999	0.999
Intraparticle diffusion	$K_{\text{diff}}(\text{mg g}^{-1} \text{min}^{-1/2})$	1.363	2.958	4.822	0.372	0.758	0.484
	$C(\text{mg g}^{-1})$	28.883	44.77	52.579	18.62	34.935	59.12
	R^2	0.904	0.960	0.936	0.817	0.730	0.832
Elovich	$\beta(\text{g mg}^{-1})$	0.159	0.0804	0.0545	0.475	0.544	0.382
	$\alpha(\text{mg g}^{-1} \text{min}^{-1})$	42.42	84.93	85.77	95.6	2899	28976
	R^2	0.976	0.976	0.957	0.923	0.940	0.930
	$q_e(\text{exp})(\text{mg g}^{-1})$	46.978	92.64	129.53	24.39	46.597	66.14

706

707 **Table 9**

708 Comparison for the removal of Auramine-O by different methods and adsorbents.

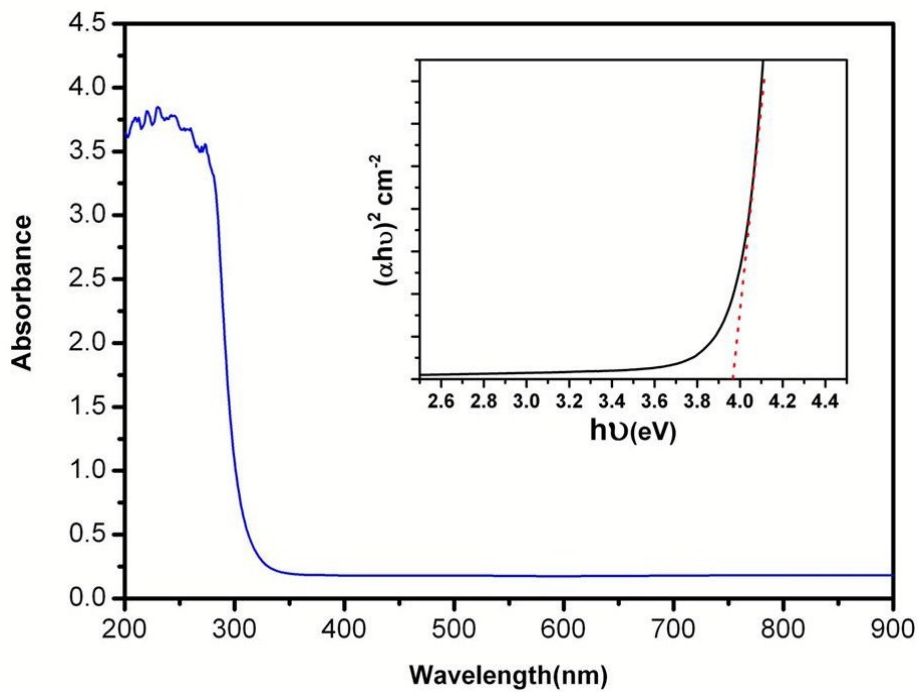
Adsorbent	adsorbent dosage (g)	dye	Concentration (mg L ⁻¹)	Contact time (min)	References
Bagasse Fly Ash (BFA)	0.001	AO	10	30-240	[77]
Activated Carbon-Commercial grade (ACC)	0.020	AO	10	120-240	[77]
Activated Carbon-Laboratory grade (ACL)	0.002	AO	10	120-240	[77]
Graphite Loaded with Titania	0.050	AO	50	300	[78]
Ag-NPs- AC	8	MB	2	16	[79]
Ag-NPs-AC	8	CR	2	6	[80]
Au-NPs-AC	10	CR	2	5	[80]
ZnS:Cu-NP-AC	0.020	AO	20	3	Proposed method

709

710

711

712



713

714 **Fig. 1.** UV-vis absorbance spectrum of the prepared ZnS:Cu-NP-AC (inset: Plot of $(\alpha h\nu)^2$ vs.
715 $h\nu$) for the prepared ZnS:Cu-NP-AC)

716

717

718

719

720

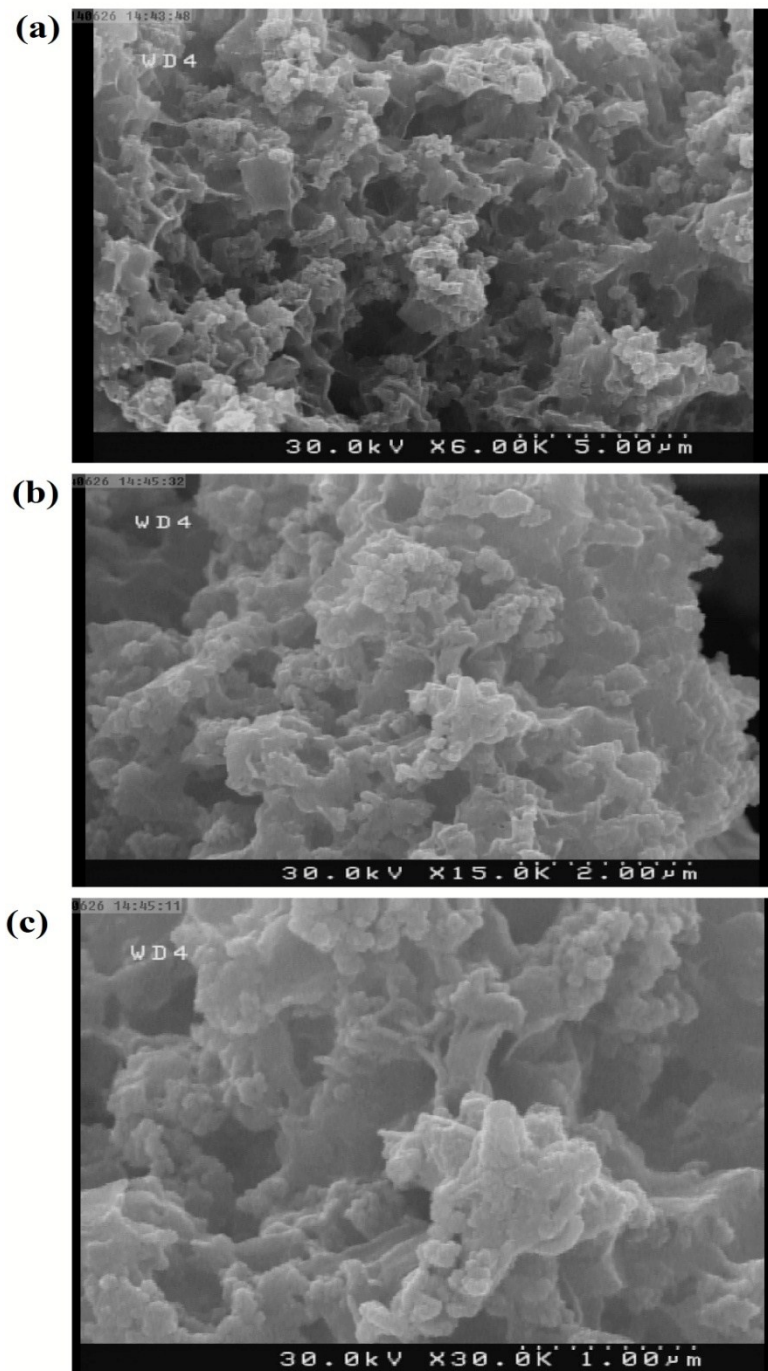
721

722

723

724

725

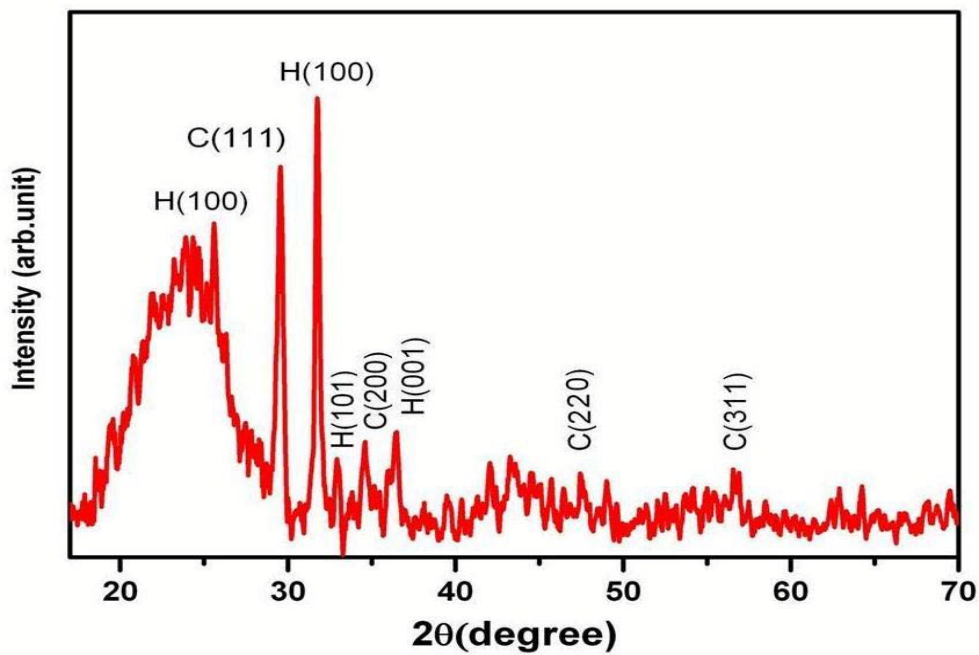


726

727 **Fig. 2.** FESEM images of the prepared ZnS:Cu-NPs-AC.

728

729



730

731 **Fig. 3.** XRD pattern for prepared ZnS: Cu-AC-NP. (H: hexagonal and C: cubic)

732

733

734

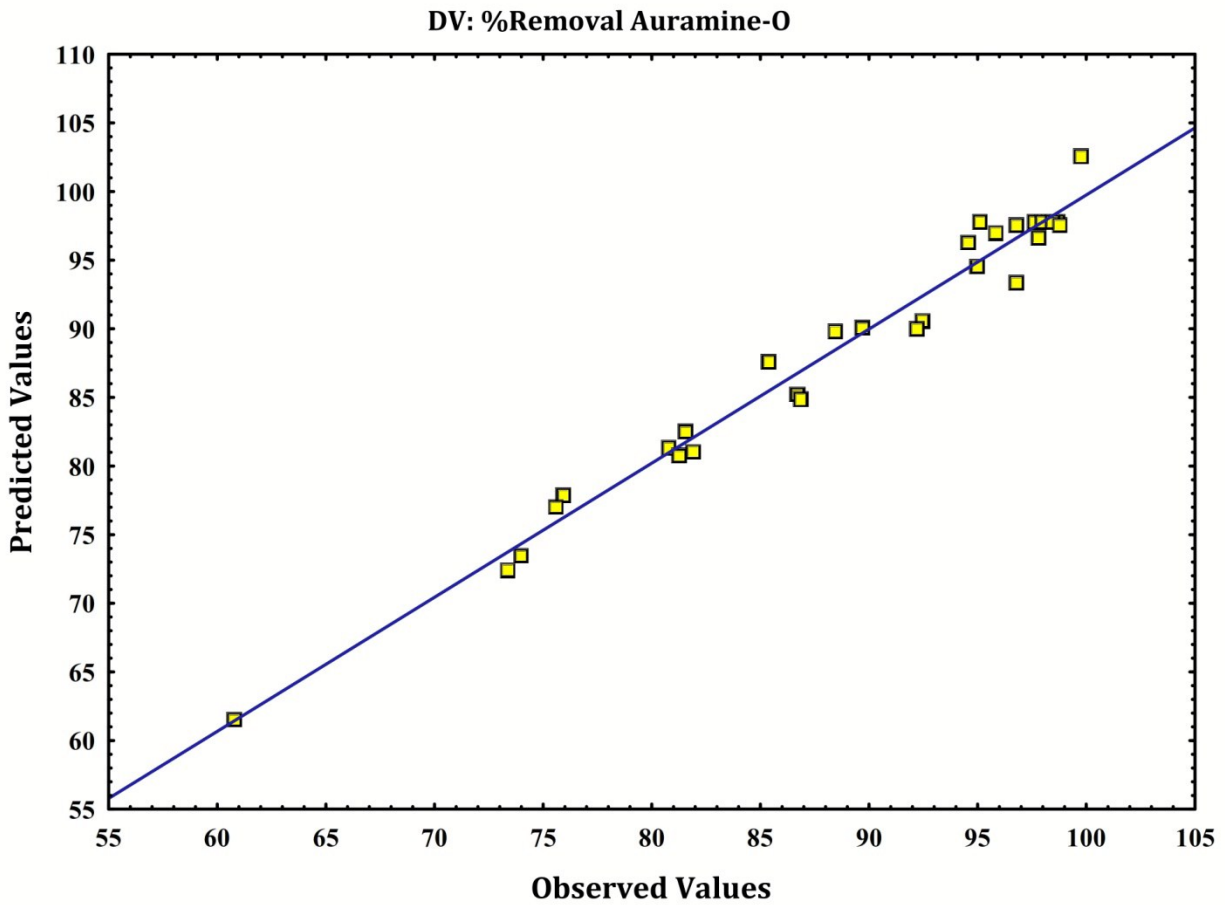
735

736

737

738

739



740

741 **Fig. 4.** The experimental data versus predicted data for removal of AO.

742

743

744

745

746

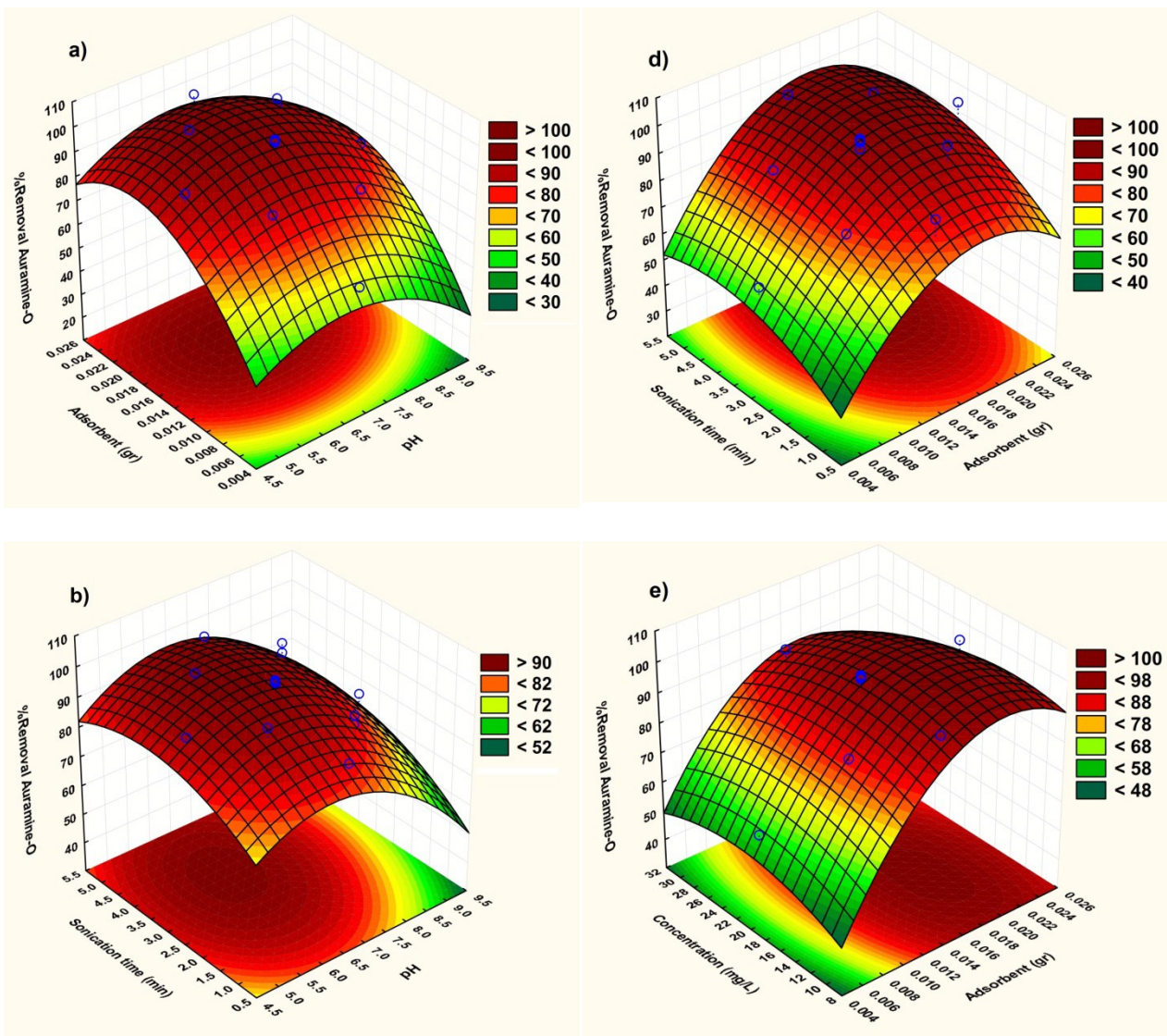
747

748

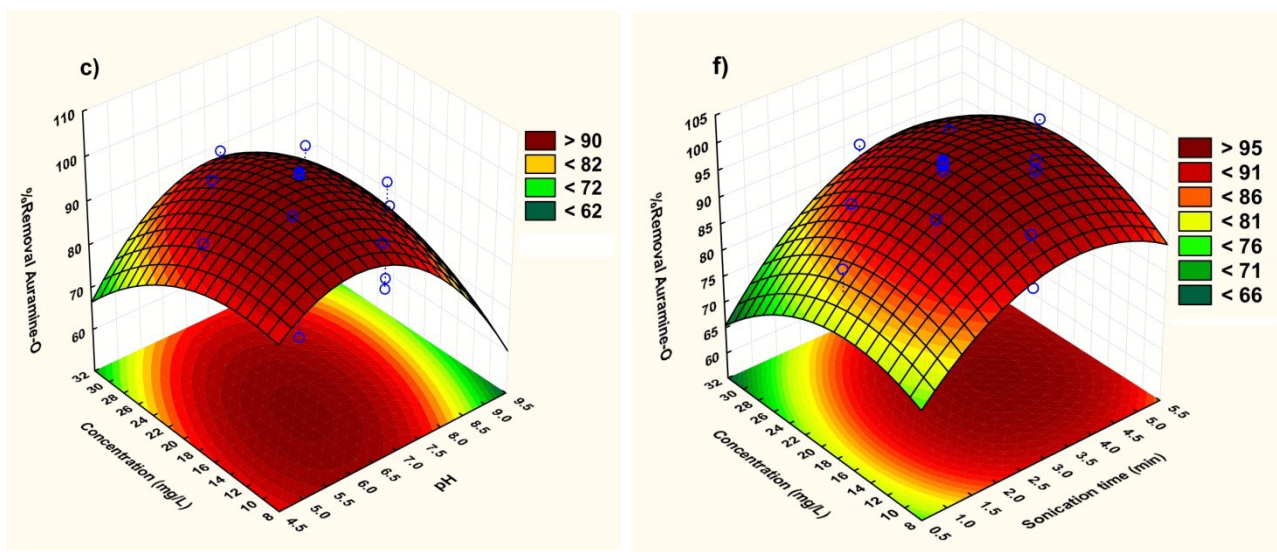
749

750

751



RSC Advances Accepted Manuscript



752

753 **Fig. 5.** Response surfaces for the AO removal: (a) X_1 - X_2 ; (b) X_1 - X_3 (c) X_1 - X_4 (d) X_2 - X_3 ; (e) X_2 -
754 X_4 and (f) X_3 - X_4 .

755

756

757

758

759

760

761

762

763

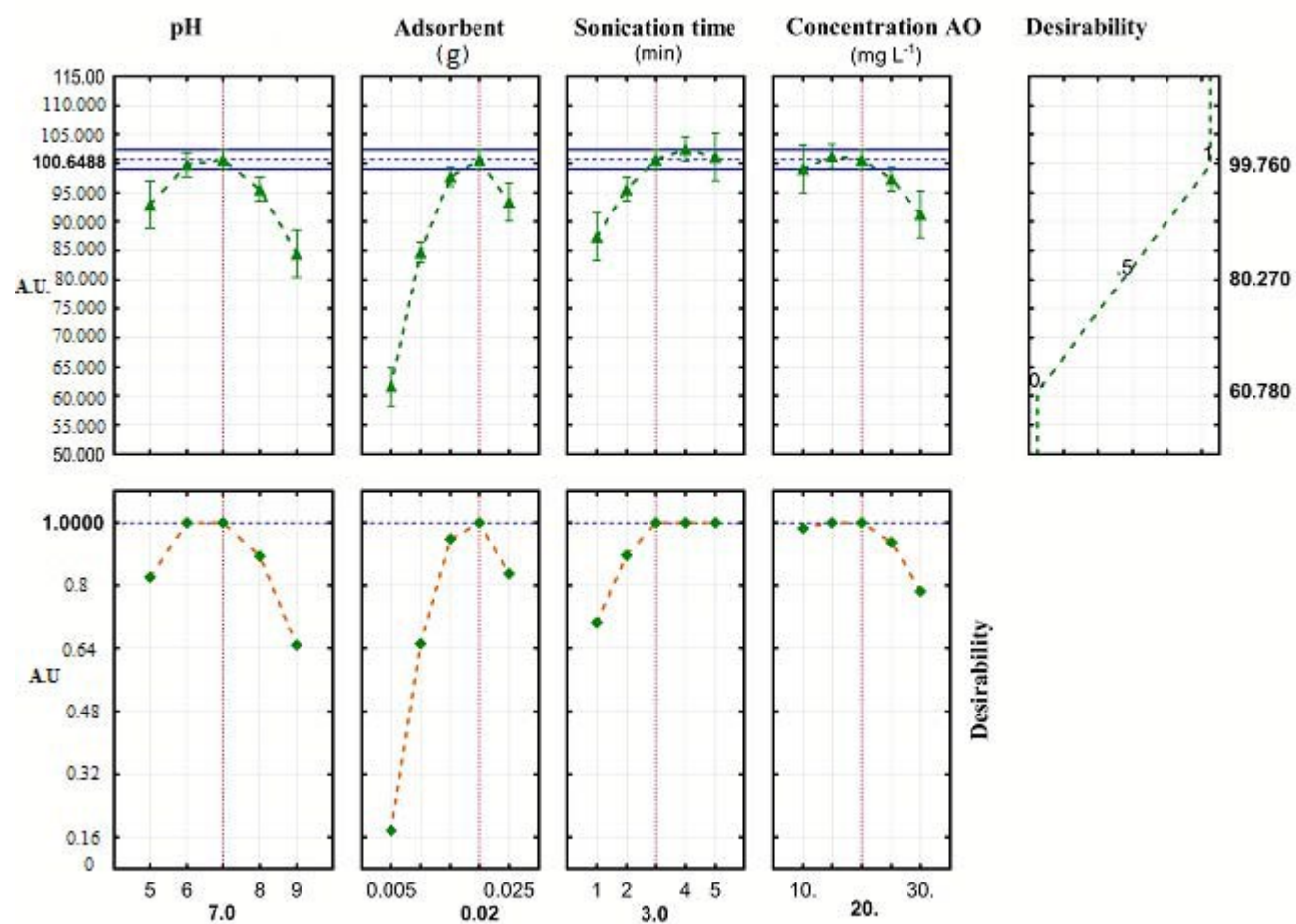
764

765

766

767

768



769

770 **Fig. 6.** Profiles for predicted values and desirability function for removal percentage of AO.

771 Dashed line indicated current values after optimization.

772

773

774

775

776

777